Thermodynamics of Triple-Helix and Double-Helix Formations by Octamers of Deoxyriboadenylic and Deoxyribothymidylic Acids

Naoki SUGIMOTO,* Yuki SHINTANI, Atsushi TANAKA,† and Muneo SASAKI
Department of Chemistry, Faculty of Science, Konan University, 8-9-1 Okamoto, Higashinada-ku, Kobe 658
(Received September 30, 1991)

The triple-helix and double-helix formations by octamers of deoxyriboadenylic and deoxyribothymidylic acids, $(dA)_8$ and $(dT)_8$, have been studied energetically and dynamically by UV and CD measurements, a melting analysis, curve-fitting and nearest-neighbor calculations. The UV mixing curves and CD spectra showed that the triple-helix of $(dA)_8 \cdot 2(dT)_8$ mainly existed in 0.05 mol dm^{-3} $MgCl_2$ buffer at a low temperature range, while the double helix of $(dA)_8 \cdot (dT)_8$ existed in 1 and 0.1 mol dm^{-3} NaCl buffers. The thermodynamic parameters for the triplex and duplex formations were obtained with analysis for the UV melting curves. The free-energy changes at 25 °C obtained from the melting temperature vs. oligomer concentration plots in the $MgCl_2$ buffer were -20.7 kJ mol^{-1} for the triplex formation and -27.3 kJ mol^{-1} for the duplex formation, respectively, which were consistent with the values obtained from the curve-fitting calculations. The free-energy changes for the duplex formation at 25 °C were -28.5 kJ mol^{-1} in 1 mol dm^{-3} NaCl buffer, and -11.6 kJ mol^{-1} in 0.1 mol dm^{-3} NaCl bufer, respectively. These values were discussed in comparison with the predicted values by the nearest-neighbor calculation.

An unusual structure of a DNA such as a triple helix is often found *in vivo* and *in vitro* though its detailed role in biology is unknown.[1] From a viewpoint of reaction, the recent works of Dervan's and Helene's groups[2–5] on the sequence-specific DNA cleavage and ligation based on triple-helix formations have led to great interest as DNA reactions in nonenzymatic systems. On the other hand, from a viewpoint of structure, it is widely believed that the triple helix is formed by major-groove binding of a polypyrimidine in parallel orientation to a polypurine segment within a DNA double helix.[6] Recently, it was reported that short oligodeoxyribonucleotides such as $(dA)_6 \cdot 2(dT)_6$,[7] $(dA)_8 \cdot 2(dT)_8$,[8] $(dA)_{10} \cdot 2(dT)_{10}$,[9] and $(dG\text{-}dA)_4 \cdot 2(dT\text{-}dC)_4$[10] were able to form the triple-helix *in vitro*. These reports gave, to our intuition, the possibility to get much information on the detailed energetics for a triple-helix formation of oligodeoxyribonucleotides.

In this work, therefore, the triple-helix ($(dA)_8 \cdot 2(dT)_8$) and double-helix ($(dA)_8 \cdot (dT)_8$) formations (Eqs. 1 and 2) by octamers of deoxyriboadenylic and deoxyribothymidylic acids, $(dA)_8$ and $(dT)_8$, have been studied energetically by UV and CD measurements, a melting analysis, curve-fitting and nearest-neighbor calculations.

$$(dA)_8 + (dT)_8 \rightleftarrows (dA)_8 \cdot (dT)_8 \text{ duplex} \quad (1)$$

$$(dA)_8 \cdot (dT)_8 \text{ duplex} + (dT)_8 \rightleftarrows (dA)_8 \cdot 2(dT)_8 \text{ triplex} \quad (2)$$

Experimental

The colon as in $(dA)_8 : 2(dT)_8$, and the plus symbol as in $(dA)_8 + 2(dT)_8$, in this paper, denote a stoichiometric ratio and a stoichiometric mixture of two DNA strands, respectively. The minibullet as in $(dA)_8 \cdot 2(dT)_8$ denotes an actual DNA structure, such as triplex or duplex, according to the previous papers.[8,9]

Materials. The octadeoxyribonucleotides, $(dA)_8$, and $(dT)_8$, were obtained from Pharmacia and purified with a high-performance liquid chromatography (HPLC) and desalted with a C-18 Sep-Pak cartridge. Final purity of the oligomers checked by HPLC was greater than 99 %. The buffer was 0.01 mol dm^{-3} sodium phosphate, pH 7.1 containing 1 or 0.1 mol dm^{-3} NaCl or 0.05 mol dm^{-3} $MgCl_2$. Oligonucleotide concentrations (C_t; total strand concentrations) were determined from a high-temperature absorbance as described previously.[11] Single-strand extinction coefficients were calculated from extinction coefficients of dinucleotide monophosphates and nucleotide.[12]

UV and CD Measurements. UV spectra, mixing curves, and melting curves (absorbance vs. temperature curves) were measured on Hitachi U-3200 and U-3210 spectrophotometers equipped with temperature controllers. At the mixing experiments, aliquots of $(dT)_8$ were added to a solution of $(dA)_8$ in a quartz cuvette. After mixing and equilibration, absorbance of the solution was measured at 260 nm and 0 °C. The cuvette-holding chamber was flushed with a constant stream of dry N_2 gas to avoid water condensation on the cuvette exterior.

At the melting experiments at 260 and 284 nm from 0 °C to 60 °C, the heating rate was 0.2 or 0.5 °C min^{-1} regulated with Hitachi SPR-7 and SPR-10 programmable temperature controllers. The cuvette-holding chamber was flushed with dry N_2 gas for the duration of the runs. Prior to dilution of the oligomers for the experiments, the buffers were degassed by heating to 90 °C for 10 min.

CD spectra were measured with a JASCO J-600 spectropolarimeter equipped with the temperature controller. Equimolar solutions of $(dA)_8$ and $(dT)_8$ were combined to give mixtures with stoichiometric ratios of either 1 : 1 or 1 : 2 $(dA)_8$ to $(dT)_8$. The ellipticities of these mixtures, as well as those of $(dA)_8$ and $(dT)_8$ alone, were measured from 220 to 320 nm at

† Current address: Household Products Res. Lab., Kao Corp., 1334 Minato, Wakayama 640.

5 °C with a constant stream of dry N_2 gas.

Thermodynamic Parameters and a Curve-Fitting Calculation. Thermodynamic parameters for the triple-helix and double-helix formations were obtained by two methods.

(1) The enthalpy, entropy, and free-energy changes of the duplex and triplex formations in Eqs. 1 and 2 (ΔH°_n, ΔS°_n, and ΔG°_n, respectively: n is 1 for the duplex formation at the $(dA)_8:(dT)_8$ mixture, 2 for the duplex formation at the $(dA)_8:2(dT)_8$ mixture, and 3 for the triplex formation at the $(dA)_8:2(dT)_8$ mixture, respectively) were determined by Eqs. 3 and 4: [8,11]

$$T_m^{-1} = (2.30\ R/\Delta H^\circ_n) \log (C_t/m) + (\Delta S^\circ_n/\Delta H^\circ_n), \quad (3)$$

$$\Delta G^\circ_n = \Delta H^\circ_n - T\Delta S^\circ_n, \quad (4)$$

where R is the gas constant, T_m is the melting temperature, T is temperature, and m are 4 for the duplex formation at the $(dA)_8:(dT)_8$ mixture, 2 for the duplex formation at the $(dA)_8:2(dT)_8$ mixture, and 6 for the triplex formation at the $(dA)_8:2(dT)_8$ mixture, respectively.

(2) Melting curves were fitted with a non-linear least-squares method[12] to three-state model since the cooperative part of the melting curves reflects the single-strand to double-helix, and double-helix to triple-helix equilibria in Eqs. 1 and 2. Since the obtained thermodynamic parameters are related to the equilibrium constants of the reaction in Eqs. 1 and 2 (K_1 and K_2, respectively) at the $(dA)_8:2(dT)_8$ mixture by Eqs. 5 and 6: [11]

$$K_1 = \exp\{(-\Delta H^\circ_1/RT) + (\Delta S^\circ_1/R)\}, \quad (5)$$

$$K_2 = \exp\{(-\Delta H^\circ_2/RT) + (\Delta S^\circ_2/R)\}. \quad (6)$$

The calculation can also give the mole fractions of single-, double-, and triple-strand species at each temperature, which is the advantage in comparison with the method (1) as described above.

Nearest-Neighbor Calculation. According to the nearest-neighbor model,[13-15] the free-energy change of the double-helix formation for non-self-complementary sequences consists of two terms; (1) a free-energy change for helix initiation associated with forming the first base pair in the duplex, and (2) a sum of propagation free energies for forming each subsequent base pair. Therefore, the stability of the oligodeoxyribonucleotide double helices can be calculated with the parameters of Breslauer et al.[13] for the helix initiation and propagation. However, their parameters, though are generally good, are not complete for some nearest-neighbor base pairs, and then the predicted stability of some sequences does not consist with the measured values.[14] In this work, therefore, the improved nearest-neighbor parameters[14,16] were used to calculate the stability of the double helix of $(dA)_8 \cdot (dT)_8$.

Results and Discussion

Recently, the structural analysis of the triple helix consisting of oligodeoxyriboadenylic and oligodeoxyribothymidylic acids, $(dA)_6 \cdot 2(dT)_6$[7] and $(dA)_{10} \cdot 2(dT)_{10}$,[9] by NMR has shown that both Watson-Crick and Hoogsteen base pairings are in the triplex form, and $MgCl_2$ stabilizes the triplex structure. However, little is currently known about the thermodynamic properties of the unusual structure in spite of its importance. In this section, we report, first, the existence of the triple and double helices of $(dA)_8 \cdot (dT)_8$ in $MgCl_2$ and NaCl buffers, respectively, by the UV mixing curves and CD spectra, and, second, discuss the thermodynamics of these helices by the results of UV melting curves, melting temperatures, and nearest-neighbor calculations.

UV Mixing Curves. Figure 1 shows the mixing curves of UV absorbance at 260 nm accompanying continuous addition of $(dT)_8$ to a fixed amount of $(dA)_8$ at either 0.1 mol dm^{-3} NaCl or 0.05 mol dm^{-3} $MgCl_2$. At 0.1 mol dm^{-3} NaCl as well as 1 mol dm^{-3} NaCl (unpublished result), the absorbance in Fig. 1a becomes minimum at an approximate 1:1 molar ratio [51.3% $(dT)_8$] of $(dT)_8$ to $(dA)_8$. It shows there is the $(dA)_8 \cdot (dT)_8$ duplex at 0.1 or 1 mol dm^{-3} NaCl. On the other hand, the point of minimum absorbance in Fig. 1b

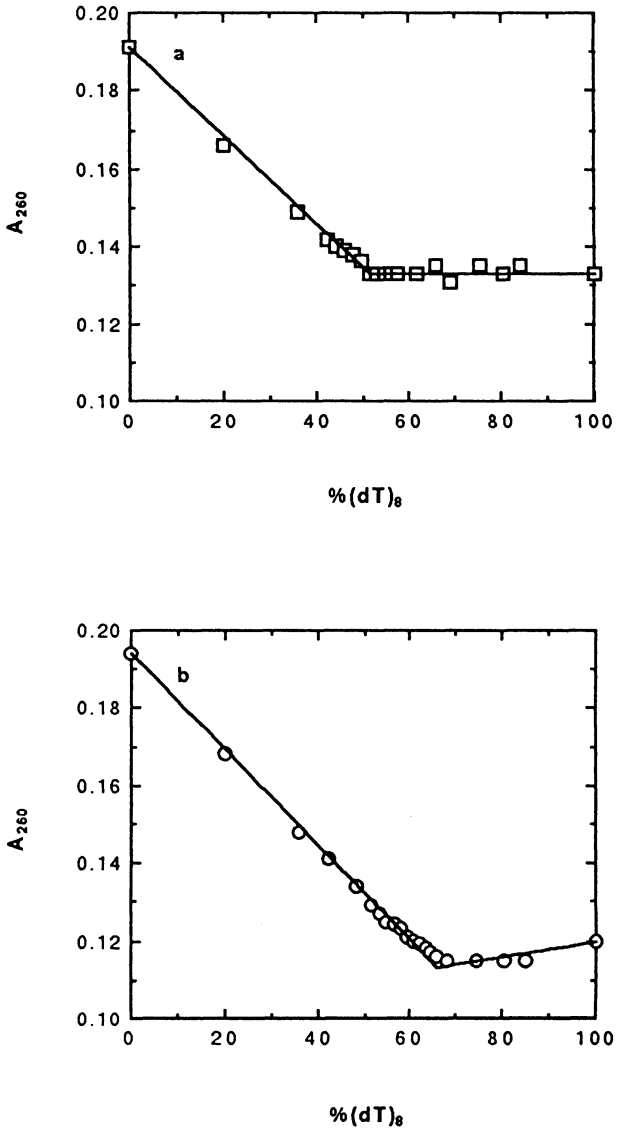

Fig. 1. Mixing curves of UV absorbance at 260 nm for reactions of $(dT)_8$ with $(dA)_8$ at (a) 0.1 mol dm^{-3} NaCl and (b) 0.05 mol dm^{-3} $MgCl_2$.

corresponds to an approximate 2 : 1 molar ratio [65.9% $(dT)_8$] of $(dT)_8$ to $(dA)_8$. The result which is similar to the result of the $(dA)_{10}+2(dT)_{10}$ system[9] suggests that there is a formation of the $(dA)_8 \cdot 2(dT)_8$ triple-helix at 0.05 mol dm^{-3} $MgCl_2$.

CD Spectra. The CD spectroscopy confirmed the presence of the $(dA)_8 \cdot 2(dT)_8$ triplex in a solution containing a 1 : 2 molar ratio $(dA)_8$: $(dT)_8$ and 0.05 mol dm^{-3} $MgCl_2$, which was consistent with the result of $(dA)_{10}$ and $(dT)_{10}$.[7] Figure 2 shows the CD spectra of a $(dA)_8+2(dT)_8$ solution containing $(dA)_8$ and $(dT)_8$ in a 1 : 2 molar ratio at 5 °C compared with the normalized sum of the CD spectra of a $(dA)_8 \cdot (dT)_8$ plus $(dT)_8$ solutions. In Fig. 2a, the CD spectrum of the $(dA)_8+2(dT)_8$ solution at 0.1 mol dm^{-3} NaCl as well as 1 mol dm^{-3} NaCl (unpublished result) is very similar to the sum of the CD spectra of the $(dA)_8 \cdot (dT)_8$ plus $(dT)_8$ solutions, suggesting there is not the triplex formation in the NaCl buffers On the other hand, in Fig. 2b, the CD spectrum of the $(dA)_8+2(dT)_8$ solution at 0.05 mol dm^{-3} $MgCl_2$ exhibits differences relative to the sum of the CD spectra of the $(dA)_8 \cdot (dT)_8$ plus $(dT)_8$ solutions, which includes a substantial amplitude decrease of the positive band at 280 nm, and blue-shifts of the positive band at 259 nm and of the negative band at 248 nm. The result, which is consistent with the result of the $(dA)_{10} \cdot 2(dT)_{10}$ triplex formatio[9] evidences that there is a $(dA)_8 \cdot 2(dT)_8$ triplex formation at 0.05 mol dm^{-3} $MgCl_2$.

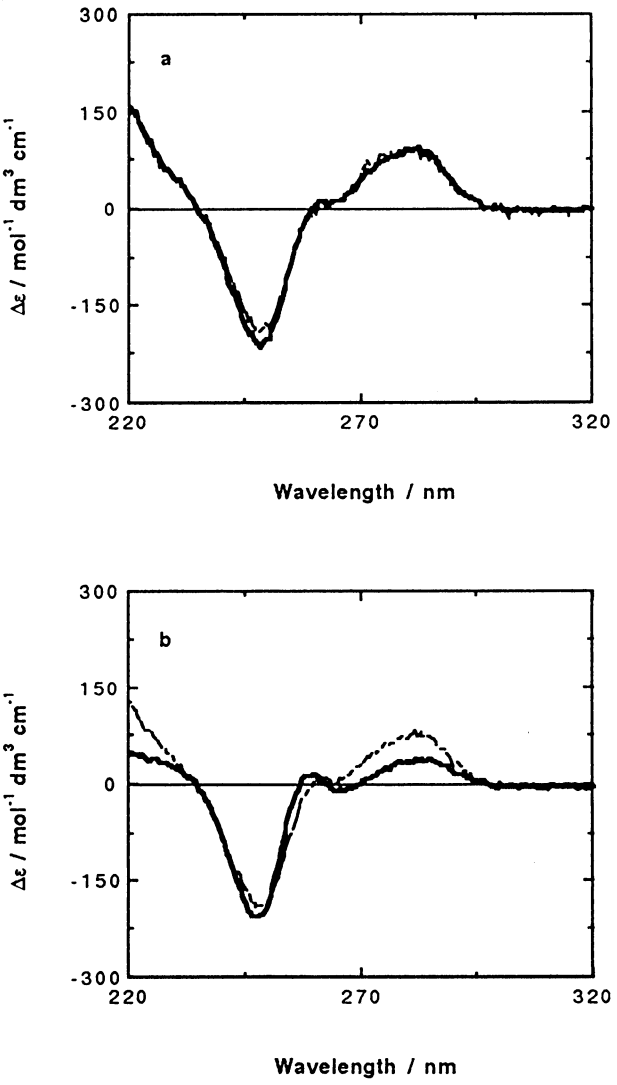

Fig. 2. CD spectra of a $(dA)_8+2(dT)_8$ solution (——) containing $(dA)_8$ and $(dT)_8$ in a 1 : 2 molar ratio in (a) 0.1 mol dm^{-3} NaCl and (b) 0.05 mol dm^{-3} $MgCl_2$ buffers at 5 °C compared with the normalized sum of the CD spectra (– – –) of a $(dA)_8 \cdot (dT)_8$ plus $(dT)_8$ solutions (1 unit of $(dA)_8$ or $(dT)_8$; 0.03 mmol dm^{-3}).

Thermodynamic Parameters of the Duplex and Triplex in $MgCl_2$ Buffer. In the previous paper[8] it was reported that the melting behavior at 284 nm was mainly due to the dissociation of the Hoogsteen base pairs, while the melting behavior at 260 nm was due to the dissociations of both the Hoogsteen and Watson–Crick base pairs. Table 1 shows the main melting temperatures, T_m, of 96.8 μmol dm^{-3} $(dA)_8 \cdot 2(dT)_8$ at each wavelength determined as described previously.[8,12,19] In Table 1, from 288 to 272 nm T_m is about 10—12 °C and constant, from 272 to 268 nm T_m increases suddenly, that is, this T_m is considered to be due to the different melting, and from 268 to 260 nm T_m is about 28—29 °C and constant, although from 268 to 260 nm the melting behavior at around 10 °C was still observed slightly. The result suggests the above idea that the dissociation of the Hoogsteen base pairs corresponds to the melting behaviors both at around 284 and 260 nm, while the dissociation of the Watson–Crick base pairs corresponds to the melting behaviors only at around 260 nm.

The melting curves were measured over a 50-fold range in the DNA concentration and the melting temperature on each run was determined. The thermodynamic parameters for the duplex and triplex formations were determined as described in the preceding experimental section. The typical plots of the reciprocal melting temperatures, T_m^{-1}, vs. log (C_t/m) in Eq. 3 are shown in Fig. 3, and the obtained thermodynamic parameters in the $MgCl_2$ buffer are listed in Table 2.

In Table 2, each thermodynamic parameter for the duplex and triplex formations obtained from the T_m^{-1}

Table 1. Melting Temperature on Each Wavelength for 96.8 μmol dm^{-3} $(dA)_8 \cdot 2(dT)_8$

Wavelength	T_m	
nm	°C	
288	10.5	
284	9.7	
280	10.4	
276	11.4	
272	12.3	
268	ca. 10[a]	28.0
264	ca. 10[a]	29.2
260	ca. 10[a]	28.8

a) The exact value was not determined.

vs. log (C_t/m) plot is consistent with the value obtained from the curve-fitting calculation within about ±10%. The free-energy changes at 25 °C in the $MgCl_2$ buffer are −20.7 kJ mol^{-1} for the triplex formation and −27.3 kJ mol^{-1} for the duplex formation, respectively, suggesting the duplex formation between $(dA)_8$ and $(dT)_8$ has the larger stability than the triplex formation between $(dA)_8 \cdot (dT)_8$ and $(dT)_8$. It may be caused not by the difference of the types of the base pairs such as the Hoogsteen and the Watson–Crick base pairs but by the difference of the conformations between the duplex and the triplex with the oligomers.[20,21]

Mole Fractions of the Single Strand, the Duplex, and the Triplex. The curve-fitting calculation gives the results of the mole fractions of the single strand, the duplex, and the triplex in the NaCl and $MgCl_2$ buffers at each temperature, and the results are shown in Fig. 4. In Fig. 4a which shows the result at 0.1 mol dm^{-3} NaCl, it is observed that the melting behavior of 0.13 mmol dm^{-3} $(dA)_8 \cdot (dT)_8$ occurs from 10 to 25 °C, and there are almost 100% of the duplex at 0 °C and the single strands above about 30 °C. On the other hand, in Fig. 4b which shows the result of 0.07 mmol dm^{-3} $(dA)_8 \cdot 2(dT)_8$ at 0.05 mol dm^{-3} $MgCl_2$, the triplex, the duplex, and the single strands exist dominantly for the temperature ranges from 0 to 20 °C, from 20 to 32 °C, and above 32 °C, respectively. It is impressive that there is no temperature at which the helix exists at 100% as the form of $(dA)_8 \cdot (dT)_8$ duplex.

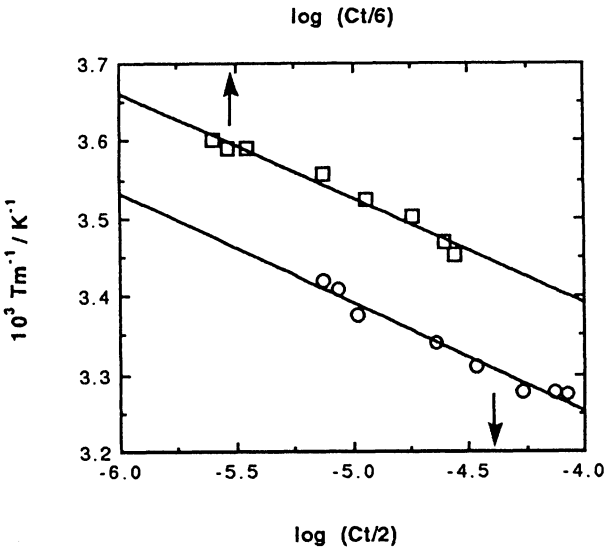

Fig. 3. Plots of T_m^{-1} vs. log (C_t/m) for $(dA)_8 \cdot 2(dT)_8$, where m are 2 for the duplex formation (○) aud 6 for the triplex formation (□), respectively.

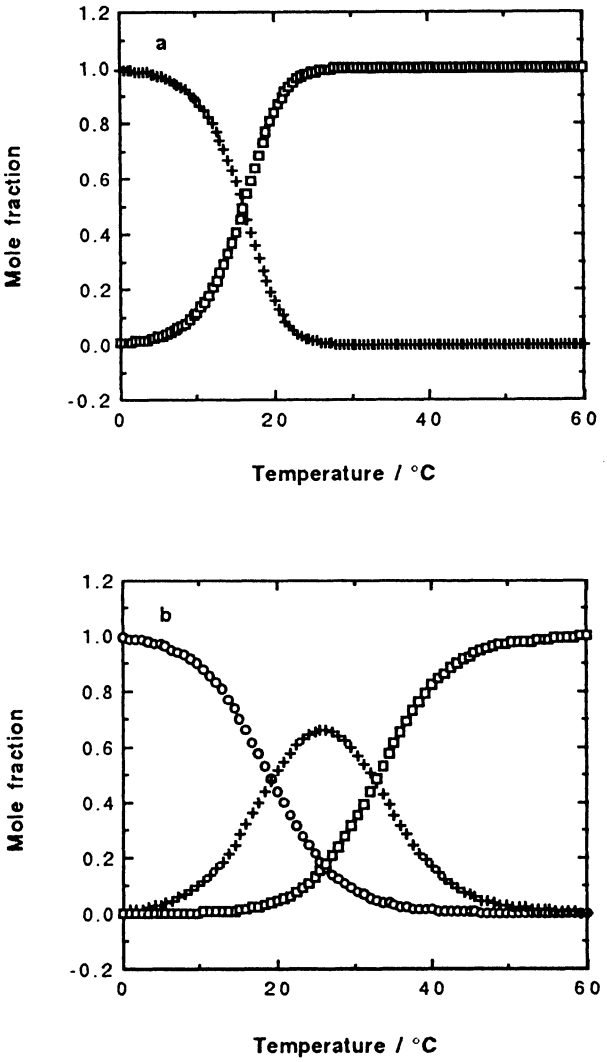

Fig. 4. Mole fractions of the single strands (□), the duplex (+), and the triplex (○) for (a) 0.13 mmol dm^{-3} $(dA)_8 \cdot (dT)_8$ in 0.1 mol dm^{-3} NaCl and (b) 0.07 mmol dm^{-3} $(dA)_8 \cdot 2(dT)_8$ in 0.05 mol dm^{-3} $MgCl_2$.

Table 2. Thermodynamic Parameters for Triple-Helix Formation of $(dA)_8 \cdot 2(dT)_8$ in 0.05 mol dm^{-3} $MgCl_2$

	n	$-\Delta H^\circ$	$-\Delta S^\circ$	$-\Delta G^\circ_{37}$	$-\Delta G^\circ_{25}$	T_m[a)]
		kJ mol^{-1}	J mol^{-1} K^{-1}	kJ mol^{-1}	kJ mol^{-1}	°C
b)	2	176	499	21.2	27.3	29.8
c)	2	124	331	21.3	25.3	26.6
b)	3	150	432	16.0	20.7	12.6
c)	3	178	530	13.6	20.0	12.4

a) The total concentration of $(dA)_8 \cdot 2(dT)_8$ is 1×10^{-4} mol dm^{-3}. b) The values were derived from the T_m^{-1} vs. log (C_t/m) plots. c) The values were derived from the curve-fitting calculation.

Table 3. Thermodynamic Parameters for Double-Helix Formation of $(dA)_8 \cdot (dT)_8$

	$[Na^+]$	$-\Delta H^\circ$	$-\Delta S^\circ$	$-\Delta G^\circ_{37}$	$-\Delta G^\circ_{25}$	T_m[a]
	mol dm^{-3}	kJ mol^{-1}	J mol^{-1} K^{-1}	kJ mol^{-1}	kJ mol^{-1}	°C
b)	1.02	250	743	19.6	28.5	27.7
c)	1.02	300	910	17.8	28.7	28.1
d)	1.02	262	786	18.4	27.9	26.8
b)	0.122	397	1293	−3.92	11.6	14.3
c)	0.122	379	1209	−4.03	18.5	19.1

a) The total concentration of $(dA)_8 \cdot (dT)_8$ is 1×10^{-4} mol dm^{-3}. b) The values were derived from the T_m^{-1} vs. log $(C_t/4)$ plots. c) The values were derived from the curve-fitting calculation. d) The values were calculated from nearest-neighbor model.

Predicted and Observed Stability of the Duplex in NaCl Buffer. Table 3 lists the thermodynamic parameters for the duplex formation in 1 and 0.1 mol dm^{-3} NaCl buffers determined by the T_m^{-1} vs. log (C_t/m) plot, the curve-fitting method, and the nearest-neighbor calculation. In 1 mol dm^{-3} NaCl buffer as well as in the $MgCl_2$ buffer, each thermodynamic parameter for the duplex formation obtained from the T_m^{-1} vs. log (C_t/m) plot is consistent with the value obtained from the curve-fitting calculation within about ±10%. These results indicate that the curve-fitting method developed in this work as well as the method of the T_m^{-1} vs. log (C_t/m) plot is very good to analyse energetics for the DNA secondary structure and has the advantage of saving the experimental time because it needs essentially the only one melting curve to be fitted. However, in 0.1 mol dm^{-3} NaCl buffer, the consistency between the values from the T_m^{-1} vs. log (C_t/m) plot and the curve-fitting calculation was not so good because the melting temperatures at low concentrations of the oligomers were very low and then the fitting calculation for the melting curves was difficult.

Current predictions of the secondary-structure stability of nucleic acids, especially oligomers, by the thermodynamic parameters for the formation of a base pairing[13–15] depend largely on the nearest neighbor model.[22,23] This model assumes that structure formations of the nucleic acids are driven by interaction between nearest-neighbor base pairs in a DNA and an RNA. The calculated thermodynamic values in 1 mol dm^{-3} NaCl buffer by the improved nearest-neighbor parameters were able to predict the experimental values in Table 1: The predicted free-energy change at 25 °C is −27.9 kJ mol^{-1} and close to −28.5 kJ mol^{-1} obtained by the plot method and −28.7 kJ mol^{-1} determined by the curve-fitting method. The predicted melting temperature is 26.8 °C and is also consistent with 27.7 and 28.1 °C obtained by the methods. When the melting temperatures of oligodeoxyribonucleotide duplexes is estimated, the nearest-neighbor method may give the more reliable value than the rule of Wallace et al.[24] by which 16 °C was predicted as the T_m of the $(dA)_8 \cdot (dT)_8$ duplex. However, the thermodynamic parameters and melting temperature calculated with the nearest-neighbor parameters at 1 mol dm^{-3} NaCl were not able to predict the experimental values at 0.1 mol dm^{-3} NaCl in Table 3, suggesting that new nearest-neighbor parameters may be needed in order to predict the stability of DNA secondary structures at different NaCl concentrations.

This work was supported in part by the Grant-in-Aid for Scientific Research on Priority Areas from the Ministry of Education, Science and Culture.

References

1) W. Saenger,"Principles of Nucleic Acid Structure," Springer, New York (1984).
2) H. E. Moser and P. B. Dervan, *Science,* **238**, 645(1987).
3) K. J. Luebke and P. B. Dervan,*J. Am. Chem. Soc.,* **111**, 8733 (1989).
4) S. A. Strobel and P. B. Dervan, *Science,* **249**, 73 (1990).
5) J.-C. Francois, T. S.-Behmoaras, M. Chassigal, N. T. Thoung, and C. Helene, *J. Biol. Chem.,* **264**, 5891 (1989).
6) R. G. Shea, P. Ng, and N. Bischofberger, *Nucleic Acids Res.,* **18**, 4859 (1990).
7) K. Umemoto, M. H. Sarma, G. Gupta, J. Luo, and R. H. Sarma, *J. Am. Chem. Soc.,* **112**, 4539 (1990).
8) N. Sugimoto, Y. Shintani, and M. Sasaki, *Chem. Lett.,* **1991**, 1287.
9) D. S. Plich, C. Levenson, and R. H. Shafer, *Proc. Natl. Acad. Sci. U.S.A.,* **87**, 1942 (1990).
10) P. Rajagopal and J. Feigon, *Nature,* **339**, 637 (1989).
11) D. H. Turner, N. Sugimoto, and S. M. Freier, "Nucleic Acids: Spectroscopic and Kinetic Data," ed by W. Saenger, Springer, Berlin (1990), Vol. 1, p. 201.
12) N. Sugimoto, A. Tanaka, Y. Shintani, and M. Sasaki, *Chem. Lett.,* **1991**, 9.
13) K. J. Breslauer, R. Frank, H. Blocker, and L. A. Marky, *Proc. Natl. Acad. Sci. U.S.A.,* **83**, 3746 (1986).
14) N. Sugimoto, K. Honda, and M. Sasaki, submitted for publication.
15) S. M. Freier, R. Kierzek, J. A. Jaeger, N. Sugimoto, M. H. Caruthers, T. Neilson, and D. H. Turner, *Proc. Natl. Acad. Sci. U.S.A.,* **83**, 9373 (1986).
16) N. Sugimoto and M. Sasaki, *Nucleosides Nucleotides,* **10**, in press (1992).
17) N. Sugimoto, N. Monden, and M. Sasaki, *Bull. Chem. Soc. Jpn.,* **63**, 697 (1990).
18) N. Sugimoto, K. Hasegawa, and M. Sasaki, *Bull.*

Chem. Soc. Jpn., **63**, 1641 (1990).
19) N. Sugimoto, R. Kierzek, and D. H. Turner, *Biochemistry*, **26**, 4554 (1987).
20) S. M. Mirkin, V. I. Lyamichev, K. N. Drushlyak, V. N. Dobrynin, S. A. Filippov, and M. D. Frank-Kamenetskii, *Nature*, **330**, 495 (1987).
21) H. Htun and J. E. Dahlberg, *Science*, **243**, 1571 (1989).
22) I. Tinoco, Jr., O. C. Uhlenbeck, and M. D. Levine, *Nature*, **230**, 363 (1971).
23) D. H. Turner, N. Sugimoto, and S. M. Freier, *Annu. Rev. Biophys. Biophys. Chem.*, **17**, 167 (1988).
24) R. B. Wallace, J. Shaffer, R. F. Murphy, J. Bonner, and K. Itakura, *Nucleic Acids Res.*, **6**, 3543 (1979).